

# Determination of a bearings operating conditions during the working process by means of BeMoS®

Christoph Brückner  
BestSens AG, Coburg, Germany  
info@bestsens.de

Sebastian Stich  
BestSens AG, Coburg, Germany

Jan Marten Behrens  
BestSens AG, Coburg, Germany

## Summary

This article gives an overview of a measurement system based on surface acoustic wave technology (SAW) to determine operation condition of bearings and there opportunity's. Bearing faults are mainly caused by bad lubrication and operation conditions. The ability to recognize these conditions, gives the possibility to counteract the fault mechanism. The technology of SAWs is integrated in BeMoS® (Bearing Monitoring System). By using special transmitter and receiver, it generates the SAWs at the bearing ring and allows a look inside the bearing. BeMoS® surveys the conditions of operation and gives the opportunity to recognize these conditions, starting from slip events in cylinder roller bearing which destroy the surfaces of the rolling contact partners, via the changes in the cinematic of spindle bearings to the contamination of water in the bearings. Additionally, BeMoS® can give the possibility to react and to adapt the maintenance or to adapt the process parameters to avoid the breakdown of bearings.

## 1. Introduction

The reliability of the production processes plays an important role in the automated manufacturing. The disruption of one step in the production can influence the whole production chain and causes downtimes. The reasons for failure are different, but a large part of interrupts are caused by bearing faults. A study form M. Wahler, an employ of SKF, described the different causes of bearing faults, most of them are related to bad lubrication and operation conditions like starvation or aging effects [1].

Figure 1 shows the causes of bearing faults and their occurrence expressed as a percentage. The ability to determine the different unsuitable operation conditions in a working process enables to counteract the faults. The manufacturers can improve their production process reliability by reducing unsuitable operations or by changing the maintenance to an appropriate servicing. Thereby a longer service life of machineries and a more reliable production process can be reached.

To fulfill this task a measurement system is needed which takes a look into the bearing and determine bad operation conditions. BeMoS® is a sensor system based on SAWs, which provides several possibilities to recognize these conditions. It can easily be integrated by putting the sensor elements on the outer bearing ring and provides the cage speed, which is an indicator for slippage or changes in the kinematic behavior, as well as an indicator for the lubrication condition in the bearing, which can be used to determine the distribution of the lubricant in the bearing. Furthermore a temperature element is integrated in each sensor element and can be evaluated to predict overheating and generate an emergency stop to save ambient parts.

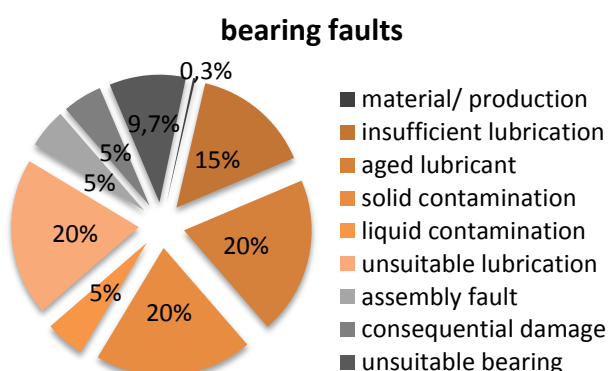


Figure 1: Causes of bearing faults [1]

Thus BeMoS® takes a look inside the bearing and provides new possibilities to measure the operation conditions. This leads to new opportunities in maintenance and process optimization.

## 2. Fundamentals

### 2.1. Bearing Technology

The operation behavior of a bearing is related to several influences, for instance the geometry of a bearing, the rotation speed, the external loads, the temperature and the lubricant. However during the working process all bearings aspire to reach the elasto-hydrodynamic lubrication (EHD or EHL). In this case the rolling contact partners are separated by a lubrication film and have no contact to each other.

Due to the rotation of the rolling contact partners the lubricant is pressed between the rolling elements and the raceway, which results in a rise of the pressure and because of the pressure-viscosity-relation to a tremendous increase of the lubricant viscosity. Beside the changes of the lubricant in the contact region the rolling contact partners are also deformed elastically. In this process a pressure distribution is generated in the contact region, which is similar to the hertzian pressure distribution, as shown in Figure 2.

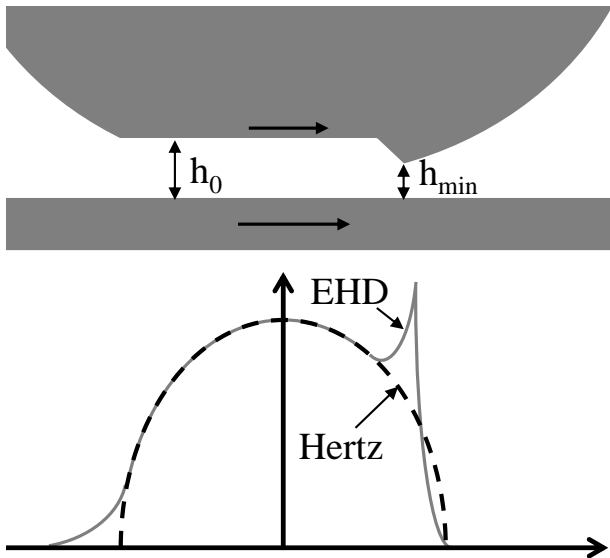


Figure 2: Pressure distribution and lubrication gap geometry in an EHD-contact

The occurring lubrication film thickness is related to the speed of the element surfaces, the viscosity, the viscosity behaviour and density of the lubricant, the geometry of the lubrication gap and the load of the contact. [2,3] Through simulations and tests Dowson and Hamrock derived the equation of the minimum lubrication fill thickness, which describes this phenomenon.[4] This is also given in the equation of the minimum lubrication fill thickness

$$h_{min} = 3,63 * U^{0,68} G^{0,49} * (1 - e^{-0,68 * K}) * R_r * w^{-0,073}$$

The cinematic of the bearing elements also plays an other important role in the bearing physics. It is necessary to ensure pure rolling at the contact region and to minimize the slide, in order to decrease the shear load in the lubricant and shear stresses at the surfaces and therefore ensure less wear of the tribological system. [5]

To guarantee minimum slide in the contact region, slip in the bearing has to be avoided. The slip rate can be calculated by the difference of the theoretical and the current cage speed.

$$S = \frac{n_{C_{theo}} - n_{C_{meas}}}{n_{C_{theo}}} = 1 - \frac{n_{C_{meas}}}{n_{C_{theo}}}$$

The cage speed is given by

$$n_c = \left( 1 \pm \cos(\phi) * \frac{D_w}{D_{pw}} \right) * \frac{n}{2}$$

By rearranging the equations a bearing parameter  $\epsilon$  can be created.

$$\epsilon = \frac{n_c}{n} = \frac{1}{2} \left( 1 \pm \cos(\phi) * \frac{D_w}{D_{pw}} \right)$$

$$\epsilon_{theo} = \frac{1}{2} \left( 1 \pm \cos(\phi) * \frac{D_w}{D_{pw}} \right); \epsilon_{meas} = \frac{n_{C_{meas}}}{n};$$

This parameter can be separated into a theoretical one, which is related to the bearing geometry and a measurable one, which is related to the current cage and shaft speed. Inserting these two parameters into the slip equation leads to

$$S = 1 - \frac{\epsilon_{meas}}{\epsilon_{theo}}$$

This slip equation can be used to value the slip rate in cylindrical roller bearings, and furthermore to value changes in the cinematic of angular ball bearings or spindle bearings. [6,7]

### 2.2. Surface Acoustic Waves

SAWs, in this case Lamb waves or Rayleigh Lamb waves are an interaction of longitudinal and vertical transversal acoustic waves. They are propagating in substrates, which are limited in the thickness. At the boundaries the longitudinal or transversal sound waves are reflected and converted in each other. Therefore propagation angles exist which provide the conversion from one to the other type of sound wave in a matching manner that a constructive superposition is created. These special cases of propagation are called modes. The modes are in general dispersive, that means the phase and group velocity depends on the frequency of the wave and thickness of the substrate. Additionally they are separated in two main types, the symmetric and antisymmetric modes, as shown in Figure 3.

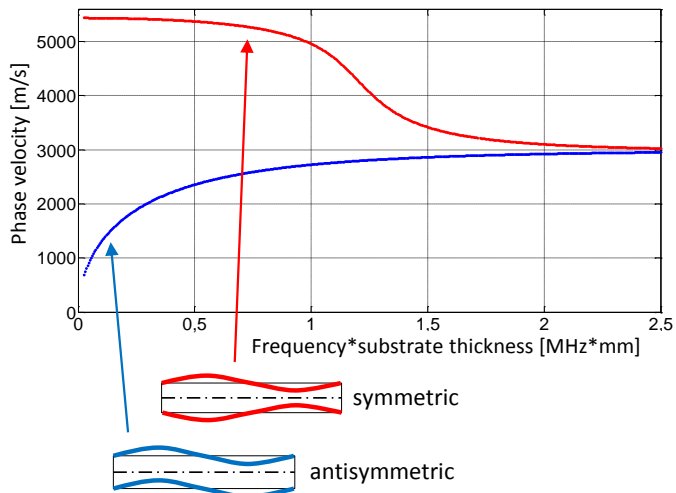


**Figure 3: Phase velocity and displacement of the basic symmetric and antisymmetric modes of steel**

This division describes the displacement of the surface to the middle of the plate, for example the symmetric modes displacement is symmetric to the middle of the plate.[8,9] In contact with a lubrication layer the propagation behaviour is changed by overcome a certain lubrication film thickness. This is caused by the transition of wave energy into the additional layer. Therefore it becomes a two layer system with an visco-elastic layer on top of an elastic substrate. [10]

Another influence of the propagation is caused by high stresses in the substrate. It leads to changes in the stress-strain relation from linear to non-linear behavior, this means higher order constants become visible. And therefore leads to a fundamental change in the propagation of sound waves which influences the behaviour of the Lamb waves.[11]

### 2.3. Application of surface acoustic waves on bearings

By using special transmitter BeMoS® generates SAWs in the outer ring of a bearing. These propagate circumferential along the outer ring and are recorded by the receiver as shown in Figure 4. The transmission of the acoustic wave is influenced by the elastic and geometric properties of the transmission line, in this case the bearing.

These properties change through the movement of the bearing elements during the rotation of the bearing.

The transmission function of the acoustic wave is modulated by each rolling element. This is caused by the ambient lubricant at the rolling element and the transferred force which changes the propagation and transmission in manifold ways, as described previous.

Out of these transmissions characteristic signal values are generated which indicate the change of the transmission function, for instance the maximum amplitude. They are recorded over the rotation of the bearing and result in a periodic signal which is evaluated in different ways, for

example the contained frequencies, the amplitude of periodic signal or the similarity of the modulations. [12]

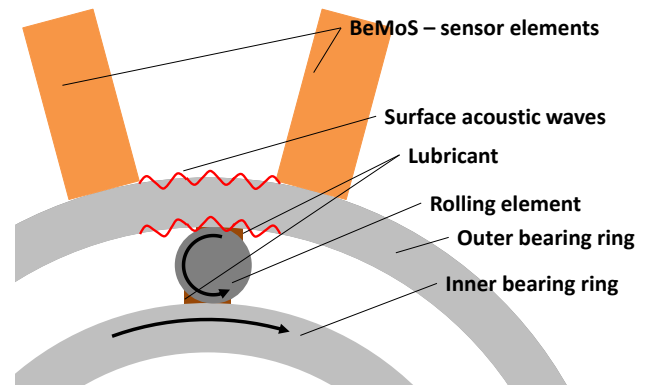


**Figure 4: Mounting of the sensor elements and structure of the transmission line**

## 3. Measurement Examples and Results

### 3.1. Slippage in a cylinder roller bearing

The used setup was built to apply different operation condition on the testing bearings. It can build up different load condition from 0 to 20 kN and rotation speeds from 0 to 15000 rpm. The setup is diagramed in Figure 5.

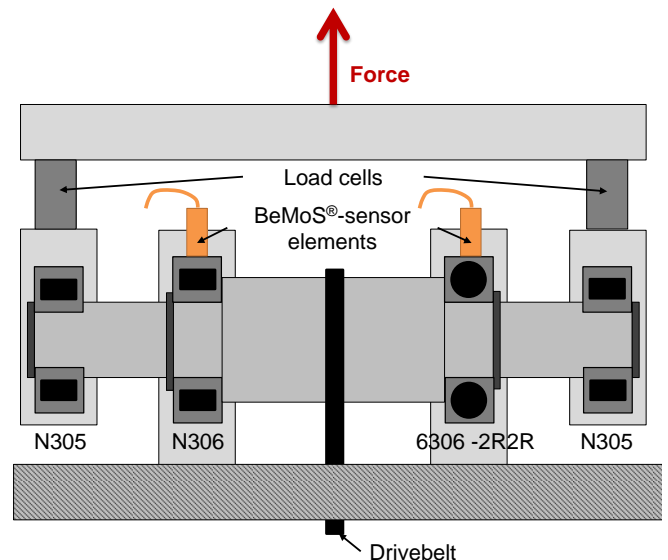


**Figure 5: schematic structure of the test-bench**

The force was measured by the load cells and the rotation speed is captured by a optical sensor element.

The measurement of the slippage behavior of the cylinder roller bearing was done by constant rotation speed. At first the high load of 1125 N was set and afterwards the load was decreased step by step to 50 N. Each step was kept for 10 minutes to come in an equilibrium state. The Figure 6 shows the measurement result for different rotation speeds. In low load regions a decreasing of the measured bearing parameter  $\epsilon$  can be observed, which results in a high deviation to the theoretical  $\epsilon$ .

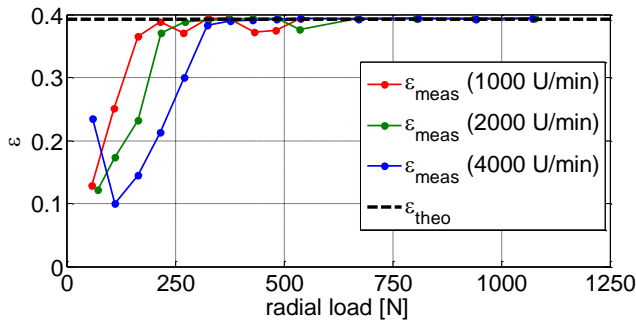


Figure 6: Bearing parameter at different operation conditions

By using the equation of the slippage the diagram can be transferred into the slip ratio of the bearing. Figure 7 shows the result of the conversion. The cylinder roller bearing has high slip rates up to 80%. This could lead to damages of the surfaces and to a failure of the bearing.

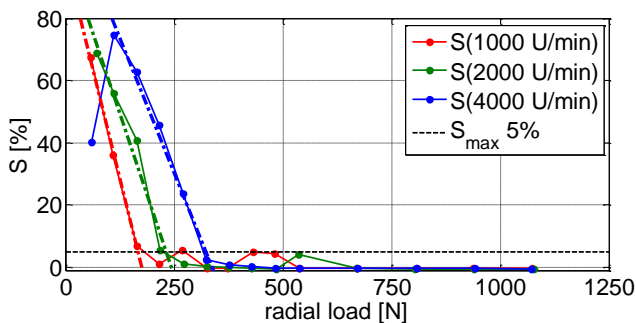


Figure 7: Slip behavior at different operation conditions

In Figure 7 is also shown a maximum permitted slip rate of 5%. Slip rates below this level are acceptable, because the harm of the surfaces are small, but slip rates above the level aren't suitable to the service time of the bearing. The increase of the slip rate in the low load region was approximated by a linear regression and the intersection between the maximum slip rate and the linear regression for each rotation speed was calculated. This intersection marks the minimum load which is needed to ensure a proper operation by the respective rotation speed.

Figure 8 shows the comparison of the measured minimum load and the guidelines from the bearing manufacturer SKF and Schaeffler.

The guidelines of the manufacturers itself have high deviation between the predicted minimum loads. The SKF model of predicting the load is closer to the measurement result than the model of Schaeffler, but it shows also deviation to the results.

To reach the highest performance of the bearings, especially by heavy cylinder roller bearings which have to fulfil a wide area of load, a measurement of the slip rate is necessary. The manufacturer models are a point of reverence, but don't use the full performance of the bearing. With BeMoS® the full performance of the bearing can be reached by suppressing slippage events and enhance the lifetime. [6]

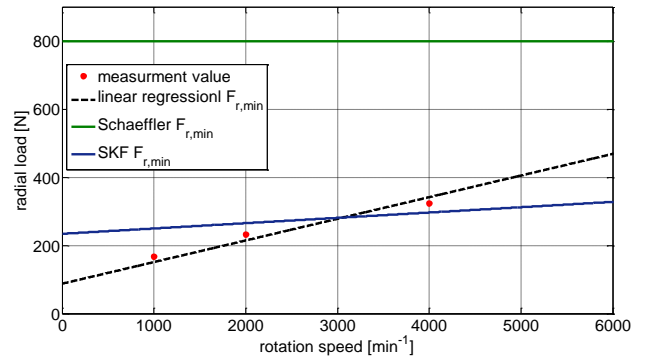


Figure 8: slip measurement results compared to the guidelines from the bearing manufacturer

### 3.2. Contamination of water

In an equilibrium state the modulation of each rolling element in the characteristic signal values are equal. Therefore each rolling element has a similar amount of lubricant and generates similar stress in the outer ring, the bearing is in a stable lubrication state. The investigation of the signal frequencies shows only certain frequencies which are related to the rotation speed of the bearing. The noise floor has no dependency on the frequency. It has a flat shape and seems to be white noise, as shown in Figure 9.a.

If water gets into a bearing, the modulation of the characteristic signal values differs from one rolling element to another. The water changes the contact region, the amount of liquid and the behavior of the liquid. These changes in the bearing can also be seen in the time signals and in the frequency spectrum, as shown in Figure 9.b. The spectrum of water contamination shows also the certain rotation frequencies, but additionally an increasing of the noise floor at low frequencies.

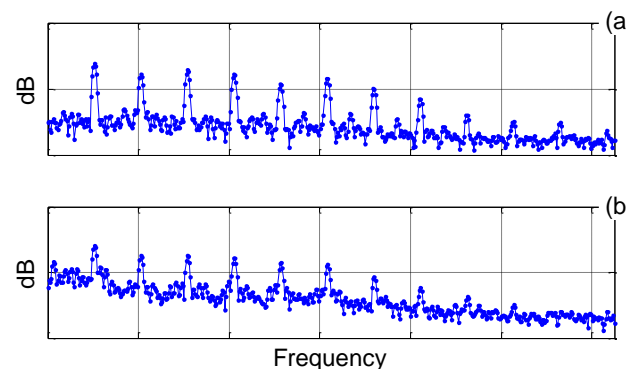
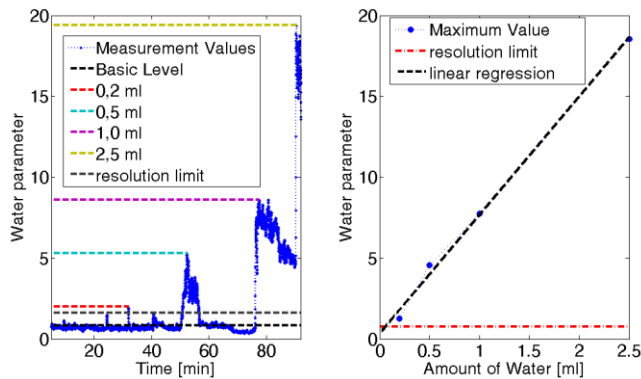


Figure 9: Frequency spectra of pure grease lubrication (a) and water contamination (b)

This increasing of the low frequency noise floor is summarized in the following as the water parameter. It is an indicator for water contamination in bearings.

The measurement was done on the same setup as mentioned in the previous chapter. The setup parameter was 200N load and 2000rpm. We examine the groove ball bearing 6306-2R2R with sealing disks. One sealing disk

was opened up by trilling to insert water. At the beginning of the test cycle the bearing has a run in process for 30 minutes to get into an equilibrium state. Afterwards every 15 minutes different amounts of water were inserting.



**Figure 10: Water parameter and the behavior by increasing amount of water in an 6306 groove ball bearing**

The transient process is shown in Figure 10 on the left side. Out of this course the maximum values of the water parameter on each state are extracted and displayed in a new diagram to examine the behavior of the water parameter in this case. It can be seen in Figure 10 on the right side, that the water parameter has a strong linear dependency to the amount of water, and is a good indicator for water contamination. In this case the minimum detectable amount of water is about 0.1 ml and corresponds to around 1% of the lubricant amount in the bearing. Other test with Schaeffler also show a good strong relationship between the water parameter and the amount of water. The reachable resolution limit is dependent on the application, especially on the bearing and the used lubricant. [13]

**3.3. Preload and kinematic in spindle bearings**

The operation behavior and cinematic of high speed bearings are an interaction of the applied forces and torques to the resulting contact pressure. In the interplay of the rotation, the forces and torques influence the movement of the rolling elements. These values change the position of the rolling element and leads to a new trajectory and contact angles of the inner and outer contact of the roller element to the raceways.

The change in the trajectory and the contact angles of the rolling elements results in a change of the bearing parameter by increasing rotation speed. Furthermore is the modification of the parameter dependent on the load of the bearing. In Figure 11 is the theoretical and measured cage speed of a 7014 hybrid bearing with a nominal contact angle of 25 degree compared with the measured cage speed.

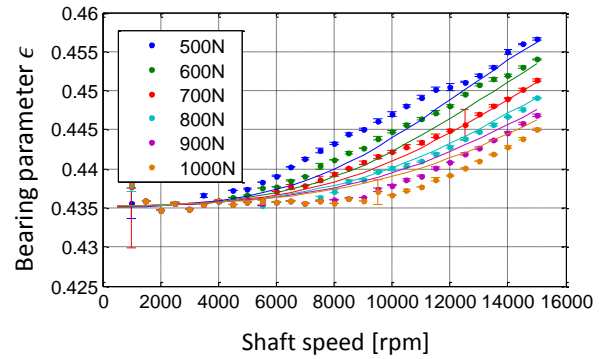


**Figure 11: Changes of the bearing parameter caused by the pre load and the rotation speed**

The diagram shows deviation between the theoretical and the measured bearing parameter in a range from about 3000 to around 13000 rpm. Before and after this region the deviation can't be observed. In Figure 12 the measured friction torque is diagrammed and shows a high increase of the momentum by low loads in a region from 2000 to 12000 rpm.

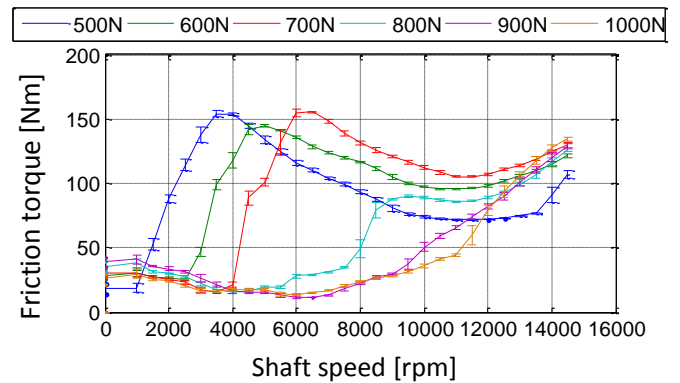


**Figure 12: Measurement of the friction torque in different operation conditions**

This results correspond to the cinematic measurements. The deviation of the loads 500N, 600N and 700N are positive, that means the measured parameter is higher than the theoretical one. In contrast to the measurement series of high loads, these have no friction torque peak and the deviation of the parameter is negative. The best fit of theoretical to measured cage speed result at a load of 800N. In which case the friction peak can be observed, but seems to be suppressed.

Thereby it appears to be a cinematic effect which arise the friction peaks. Possible explanations can be the occurrence of slip in the bearing by low loads or the difference in the shifting off the rolling element. Further investigation has to clarify this task. [7]

**4. Conclusion**

The operation behavior of bearings is related to different exogenous values, like the applied force or the rotation speed. These exogenous values define the operation

condition of a bearing which has deal with it. In a normal case these exogenous values don't lead to damages or faults of bearings, but if these values leaf the suitable and predicted level, it will come to bearing failure. BeMoS® surveys the operation condition and give the opportunity to recognize these conditions, starting from slip events in cylinder roller bearing which destroy the surfaces of the rolling contact partners, via the change in the cinematic of spindle bearings to the contamination of water in the bearings. In addition to observing bad operation conditions BeMoS® can give the possibility to react and adapt the maintenance or to adapt the process parameters to avoid the breakdown of bearings.

### List of Abbreviations

$U$	Speed parameter; $U = \eta_0 * \frac{v}{E' * R_r}$
$G$	Material parameter; $G = \alpha * E'$
$w$	Load Parameter; $w = \frac{Q}{E' * R_r^2}$
$K$	semi axis ratio of contact region
$\alpha$	Presser-Viscosity-Coefficient; [ $m^2/N$ ]
$\eta_0$	Dynamic Viscosity; [ $Pa*s$ ]
$v$	Mean Velocity; $v = \frac{v_1 + v_2}{2}$
$v_1$	Velocity of the rolling element
$v_2$	Velocity of the raceway
$E'$	Effective Young's Modulus; $E' = \frac{E}{1 - \mu^2}$
$E$	Young's Modulus; Steel=2.08e11 [ $N/m^2$ ]
$\mu$	Poisson Ratio, Steel=0.3
$R_r$	Reduced Radius
$Q$	Load of the rolling element
$S$	Slippage of cage
$n_{c_x}$	Cage speed, [rpm]
$\phi$	Effective contact angle, [ $^\circ$ ]
$D_w$	Diameter of the rolling element; [m]
$D_{pw}$	Trajectory of the rolling elements; [m]
$n$	Rotation speed of the inner bearing ring; [rpm]
$\epsilon_x$	Bearing Parameter

### List of References

- [1] Wahler M.: Schmierung bestimmt die Lebensdauer. In: Antriebs Praxis. 2006, Nr. 1, S. 38-41.
- [2] Wiśniewski, M.: Elasto-hydrodynamische Schmierung, Renningen: expertverlag, 2000
- [3] Ramsey, G.: Elasto-hydrodynamics, second edition, London: Imperial College Press, 2001
- [4] Brändlein, Eschmann, Hasbargenm, Weigand: Die Wälzlagerpraxis, 2. Auflage, Mainz: Vereinigte Fachverlage, 2009
- [5] Nakajima, A.; Mawatari, T.: Effect of Slip Ratio on Rolling Contact Fatigue of Bearing Steel Rollers lubricated with Traction Oil
- [6] Brückner, Ch.; Miedl, J.; Behrens, J.: Ermitteln des Schlupfverhaltens von Zylinderrollenlager bei unterschiedlichen Betriebsbedingungen; GFT Fachtagung, Göttingen. 2014.

- [7] Brecher, C.; Fey, M.; Brückner, Ch.; Falker, J.: Überwachung des Betriebszustandes von Wälzlagern mittels akustischer Oberflächenwellen. In: Sensor und Messsysteme, Nürnberg. 2014.
- [8] Auld, B.A.: Acoustic Fields and Waves in Solids Volume I+ Volume II, second edition, Malabar: Krieger Publishing Company, 1990
- [9] Rose, J.L.: Ultrasonic Waves in Solid Media, New York: Cambridge University Press, 2004
- [10] Bause, F.; Brückner, C.; Miedl, J.; Henning, B.: Model based sensitivity analysis of Leaky-Lamb wave propagation to the variation of viscous lubricant properties. In: Sensor und Messsysteme, Nürnberg. 2014.
- [11] Gandhi, N.; Michaels, J.E.; Lee, S.J.: Acoustoelectric Lamb Wave Propagation in a Homogeneous, Isotropic Aluminum Plate. In: Review of Progress in Quantitative Nondestructive Evaluation Volume 30; AIP Conf. Proc. 2011, S. 161-168
- [12] Lindner, G.; Brückner, Ch.; Schmitt, M.: Online bearing lubricant sensing by mode conversion of surface acoustic waves. In: SENSOR Proc.. 2011, S. 55-60.
- [13] Brückner, Ch.; Miedl, J.; Diller, W.: Erkennen von flüssigen Verunreinigungen in Wälzlagern. In: AKIDA 2014.